2-2008

# Automated bead-trapping apparatus and control system for single-molecule DNA sequencing

Gregory Bashford
*University of Nebraska-Lincoln*, gbashford2@unl.edu

Don Lamb
*LI-COR Biosciences, Inc., Lincoln, NE*

Dan Grone
*LI-COR Biosciences, Inc., Lincoln, NE*

Bob Eckles
*LI-COR Biosciences, Inc., Lincoln, NE*

Kevin Kornelsen
*Micralyne Inc., Edmonton, Alberta*

***See next page for additional authors***

**Authors**
Gregory Bashford, Don Lamb, Dan Grone, Bob Eckles, Kevin Kornelsen, Lyle Middendorf, and John Williams

# Automated bead-trapping apparatus and control system for single-molecule DNA sequencing

**Greg Bashford[1]*, Don Lamb[2], Dan Grone[2], Bob Eckles[2], Kevin Kornelsen[3], Lyle Middendorf[2], and John Williams[2]**

[1]*Department of Biological Systems Engineering, University of Nebraska-Lincoln, Lincoln, NE 68583, USA*
[2]*LI-COR Biosciences, Inc., Lincoln, NE 68504, USA*
[3]*Micralyne Inc., Edmonton, Alberta, Canada T6N 1E6*
[*] *Corresponding author: gbashford2@unl.edu*

**Abstract:** We have been investigating a microfluidics platform for high-speed, low-cost sequencing of single DNA molecules using novel "charge-switch" nucleotides. A significant challenge is the design of a flowcell suitable for manipulating bead-DNA complexes and sorting labeled polyphosphate molecules by charge. The flowcell is part of a single-molecule detection instrument, creating fluorescence images from labeled polyphosphates. These images would ultimately be analyzed by signal processing algorithms to identify specific nucleotides in a DNA sequence.

Here we describe requirements of the fluidics system for loading, identifying, tracking, and positioning beads. By dynamically modulating pressure gradients in the plenum chambers of a multi-channel network, we could guide individual beads with high precision to any desired coordinate and reversibly trap them in stepped channels. We show that DNA immobilized on pressure-trapped beads can be physically extended into a downstream channel under electric force for analysis. Custom dynamic algorithms for automated bead control are described.



**OCIS codes:** (070.0070) Fourier optics and signal processing; (100.0100) Image processing; (120.0120) Instrumentation, measurement, and metrology; (170.0170) Medical optics and biotechnology; (180.0180) Microscopy

## References and links

1. L. M. Davis, E. R. Fairfield, C. A. Harger, J. H. Jett, J. H. Hahn, R. A. Keller, L. A. Krakowski, J. C. Martin, B. L. Marrone, R. L. Ratliff, N. K. Seitzinger, E. B. Shera, and S. A. Soper, "High-speed DNA sequencing - an approach based upon fluorescence detection of single molecules," abstracts of papers of the American Chemical Society **200**, 75-ANYL (1990).
2. L. T. Franca, E. Carrilho, and T. B. Kist, "A review of DNA sequencing techniques," Q. Rev. Biophys. **35**, 169-200 (2002).
3. J. H. Jett, R. A. Keller, J. C. Martin, N. K. Seitzinger, and E. B. Shera, "Single molecule detection in flowing sample streams as an approach to DNA sequencing," abstracts of papers of the American Chemical Society **198**, 41-ANYL (1989).
4. J. Stephan, K. Dorre, S. Brakmann, T. Winkler, T. Wetzel, M. Lapczyna, M. Stuke, B. Angerer, W. Ankenbauer, Z. Foldes-Papp, R. Rigler, and M. Eigen, "Towards a general procedure for sequencing single DNA molecules," J. Biotechnol. **86**, 255-267 (2001).
5. J. G. K. Williams and G. R. Bashford, "Single molecule detection systems and methods," U.S. Patent 7,118,907 (10-10-2006).
6. J. G. K. Williams, G. R. Bashford, J. Chen, D. D. Draney, N. Narayanan, B. Reynolds, and P. Sheaff, "Charge-switch nucleotides," U.S. Patent 6,936,702 (8-30-2005).
7. J. G. K. Williams and G. R. Bashford, "Nucleic acid sequencing using charge-switch nucleotides," U.S. Patent 6,869,764 (3-22-2005).
8. C. M. Frey, J. L. Banyasz, and J. E. Stuehr, "Interactions of divalent metal ions with inorganic and nucleoside phosphates. II. Kinetics of magnesium(II) with HP 3 O 10 4- ,ATP, CTP, HP 2 O 7 3- , ADP, and CDP," J. Am. Chem. Soc. **94**, 9198-9204 (1972).
9. H. Kojima, E. Muto, H. Higuchi, and T. Yanagida, "Mechanics of single kinesin molecules measured by optical trapping nanometry," Biophys. J. **73**, 2012-2022 (1997).

#90526 - $15.00 USD Received 6 Dec 2007; revised 23 Jan 2008; accepted 25 Jan 2008; published 29 Feb 2008

10. S. C. Kuo and M. P. Sheetz, "Force of single kinesin molecules measured with optical tweezers," Science **260**, 232-234 (1993).
11. A. D. Mehta, M. Rief, J. A. Spudich, D. A. Smith, and R. M. Simmons, "Single-molecule biomechanics with optical methods," Science **283**, 1689-1695 (1999).
12. C. Gosse and V. Croquette, "Magnetic tweezers: micromanipulation and force measurement at the molecular level," Biophys. J. **82**, 3314-3329 (2002).
13. J. C. McDonald, D. C. Duffy, J. R. Anderson, D. T. Chiu, H. Wu, O. J. Schueller, and G. M. Whitesides, "Fabrication of microfluidic systems in poly(dimethylsiloxane," Electrophoresis **21**, 27-40 (2000).
14. J. W. Goodman, *Introduction to Fourier Optics*, (Roberts and Co., 2004).
15. R. C. Gonzalez and R. E. Woods, *Digital Image Processing*, (Addison-Wesley Reading, Mass, 1987).
16. A. C. Kak, M. Slaney, and G. Wang, "Principles of computerized tomographic imaging," Med. Phys. **29**, 107 (2002).
17. J. J. D'Azzo and C. D. Houpis, *Linear Control System Analysis and Design: Conventional and Modern*, (McGraw-Hill Higher Education, 1995).

## 1. Introduction

Single-molecule sequencing has several advantages over current sequencing methods [1-4]. It eliminates the need for cloning along with the associated large-scale laboratory automation infrastructure; it promises reads lengths of tens of kilobases; and it enables the possibility of increased sequencing throughput with reduced sequencing costs. If such a technology were successfully developed, these attributes would enable applications that are not feasible using current sequencing methods. We have investigated an "electrosorting" system for real-time single molecule DNA sequencing [5-7]. System components include modified nucleotides, an adapted DNA polymerase, a method for docking beads to which DNA template molecules are attached, a microfluidics flowcell for sorting molecules by charge, and a microscope for imaging individual fluorescent dye labeled molecules.

We have developed "electrosorting" chemistry for single-molecule sequencing based on novel "charge-switch" nucleotide triphosphates (γ-dNTPs). In a γ-dNTP, a fluorescent dye is attached by a linker to the γ-phosphate. In the example γ-dGTP species shown in Fig. 1(a), the linker has an elementary charge of (+2) and the three phosphates (-3), for a net charge of (-1). At high concentrations of Mg++, this divalent cation coordinates to the phosphates, which causes the net charge to change from (-1) to (+1). At intermediate Mg++ concentrations, the net charge can be modulated between (-1) and (+1) by adjusting Mg++ concentration. When incorporated into DNA by polymerase, pyrophosphate is naturally cleaved from the nucleotide; and in our case the pyrophosphate "PPi" is labeled with a fluorophore "F" [Fig. 1(b)]. Same as the intact γ-dNTP, the net charge of the PPi-F species is (-1) in the absence of Mg++, switching to (+1) in the presence of Mg++. However, since terminal phosphates are known to bind Mg++ with greater affinity than phosphodiester phosphates [8], it should be possible to differentially modulate the net charges of the intact nucleotide and labeled pyrophosphate species by adjusting the Mg++ concentration.

By establishing a net charge difference between the γ-dNTP and the PPi-F, it should be possible to sort the two species in an electric field (Fig. 2). This concept of sequencing DNA involves a single polymerase-DNA complex immobilized on a bead trapped near a "tee" intersection (Fig. 3). An electric field at the intersection draws intact fluorescent and positive charged γ-dNTPs toward the negative electrode while the fluorescent and negative charged PPi-F molecules move in the opposite direction where they are detected. It would be necessary for each of the four types of nucleotides to be labeled with a different dye to enable real-time sequencing as successive PPi-F molecules stream one-by-one into the detection channel. By sorting molecules in this manner, the cleaved PPi-F molecules are detected at a geometric location separate from that location of unincorporated γ-dNTPs.

A significant challenge is the design and construction of a microfabricated flowcell suitable for sorting and detecting single charge-switch nucleotides, to be used for this method of sequencing. A key feature of the microfluidics system in our sequencing scheme is the requirement of independent control of bulk fluid flow and electrophoresis. Charge-switch nucleotides would be moved and separated throughout the flowcell by application of electric

#90526 - $15.00 USD Received 6 Dec 2007; revised 23 Jan 2008; accepted 25 Jan 2008; published 29 Feb 2008

fields; however, simultaneously the application of pressure (bulk fluid flow) would hold a bead-DNA complex in place. Electroosmotic flow (EOF) effectively couples the electric field to bulk fluid flow and is thus undesirable in our system. This sequencing scheme requires the "trapping" or positioning of small polymer beads into a "cove" or pocket close to the sorting intersection. Although alternative bead manipulation techniques involving optical [9-11] and magnetic [12] forces have been utilized, our application is simplified by using pressure gradients only. In addition, to optimize sequencing throughput, a robust automated method must be developed to sequentially load and unload multiple beads from their associated traps.

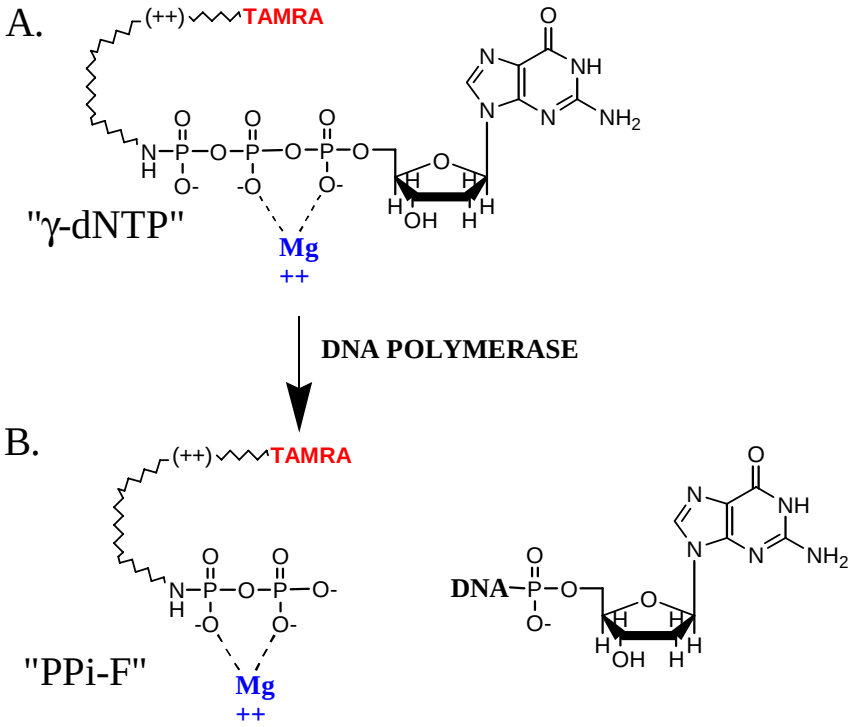


Fig. 1. Charge-switch nucleotide. (A) dGTP is phosphate-labeled with a linker and a TAMRA dye. The linker has two quaternary amino groups (++) which confer an elementary charge of +2. The label is TAMRA (Invitrogen), a zwitterionic fluorophore contributing zero net charge. (B) Labeled pyrophosphate PPi-F is cleaved from the nucleotide by polymerase. This creates a "terminal phosphate" with an ionizable oxygen giving the PPi-F a stronger interaction with Mg++ as compared to the intact γ-dNTP.

#90526 - $15.00 USD Received 6 Dec 2007; revised 23 Jan 2008; accepted 25 Jan 2008; published 29 Feb 2008

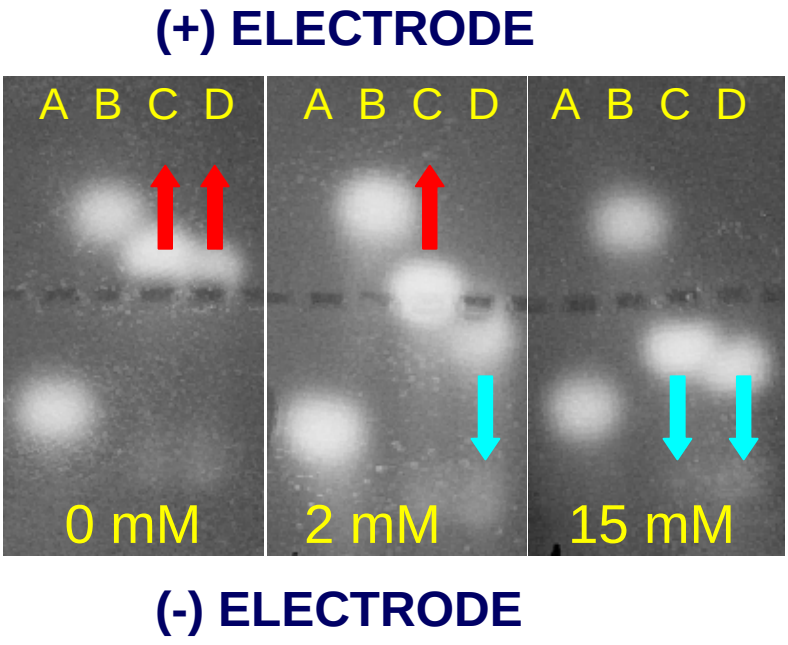


Fig. 2. Electrosorting on the basis of differential affinity for $Mg^{++}$. Lane A = TAMRA amine (charge +1), lane B = TAMRA carboxylate (charge -1), lane C = g-dTTP, lane D = PPi-F. The structures of g-dTTP and PPi-F are similar to the dGTP analogs shown in Fig. 1. Samples were resolved by electrophoresis in a 5% agarose gel containing the indicated concentrations of Mg++ (0, 2 and 5 mM). As implied by Fig 1, the net charges of the g-dTTP and the PPi-F are differentially sensitive to Mg++ concentration.

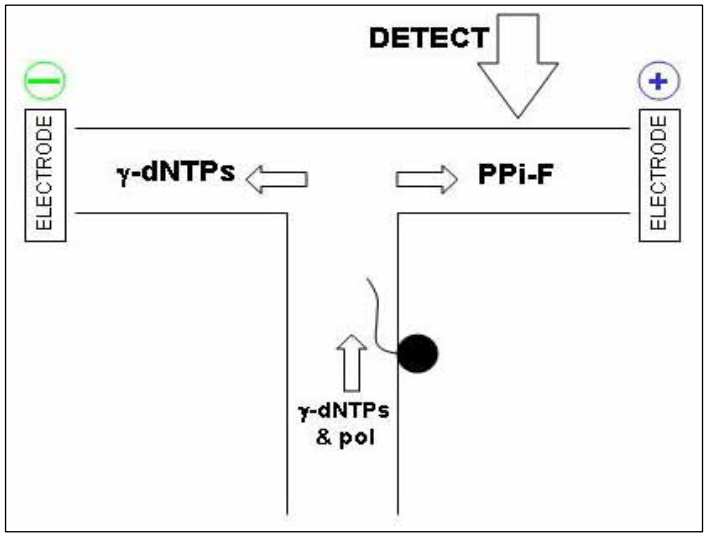


Fig. 3. Scheme for single-molecule sequencing by electrosorting. The target DNA strand is immobilized on a bead trapped in a microchannel (trap design not shown). Pressure-driven flow moves polymerase and all 4 γ-dNTPs past the DNA as indicated (vertical arrow). Nucleotide incorporation generates labeled pyrophosphate PPi-F. An electric field in the horizontal channel drives intact γ-dNTPs to the left and PPi-F to the right where it is detected by fluorescence. A shallow channel depth (0.5um) and total internal reflectance optics provide efficient detection of single molecules.

#90526 - $15.00 USD Received 6 Dec 2007; revised 23 Jan 2008; accepted 25 Jan 2008; published 29 Feb 2008

## 2. Materials and methods

### *2.1 DNA loading of beads*

Streptavidin-coated 2.8µ beads (Bangs Laboratories, Fishers, IN) were used to transport DNA throughout the flowcell. A piece of lambda DNA was ligated to a dual-biotinylated oligonucleotide. The biotinylated DNA was incubated with the streptavidin-coated beads at a 1000:1 ratio in a pH 7.8 buffer with sodium chloride and 0.1% Tween. Most beads were coated with a great deal of DNA which was visualized using the intercalating dye, SYBR GREEN, (Molecular Probes; Eugene, OR) under a fluorescent microscope.

### *2.2 Flowcell design*

An obvious advantage of DNA sequencing on a chip is the flexibility to incorporate multiple sequencing sites in a small area. While investigating different designs, a "spoked wheel" flowcell design was conceived (Fig. 4) that utilizes 10 separate bead docking and electrosorting areas with a common nucleotide source (the rim of the wheel) and drain for incorporated nucleotides (center of the wheel), respectively. Figure 4 shows a SEM photograph of the wheel flowcell without the electrosorting channels. The purpose of this flowcell was to experiment with hydrodynamic pressures, finding conditions suitable for the introduction and retention of beads, in a flowcell constructed of materials consistent with the expected final design.

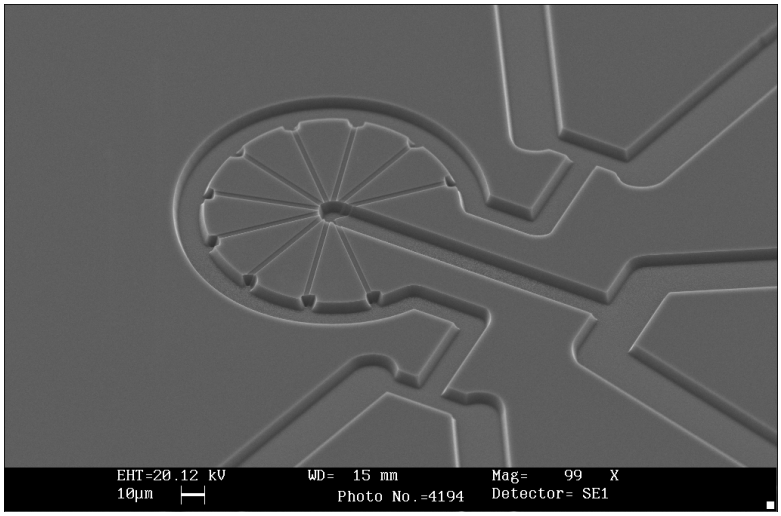


Fig. 4. SEM picture of flowcell. Wheel flowcell network design cast from a silicon master.

Two versions of the wheel flowcell were produced. The first version was composed of a SOI (Silicon On Insulator) base plate and a Pyrex coverslip. The SOI base plate was composed of three layers: 1) a device layer 12 um thick with 800-1200 ohm-cm resistivity, 2) an oxide layer 1 um thick, and 3) a handle wafer of 400 um thickness and 1-10 ohm-cm resistivity. The flowcell features were etched into the device layer of the silicon base plate. The silicon channel etch depths were 4 um for the wide channels (wheel rim, supply, and drain) and 0.5 um for the detection channel. The coverslip was 7740 Pyrex glass with nominal thickness of 160 um, anodically bonded to the silicon. Before bonding, the etched base plate was oxidized (119 nm thick) in order to electrically insulate the channels. Access holes were created by DRIE, leaving ports approximately 300 um wide.

The second version of the wheel flowcell was composed of polydimethylsiloxane (PDMS), for ease of production [13]. The PDMS was cast against a silicon "master", with bas-relief features created by lithography methods. A silicon wafer was oxidized to 140 nm,

#90526 - $15.00 USD Received 6 Dec 2007; revised 23 Jan 2008; accepted 25 Jan 2008; published 29 Feb 2008

followed by photoresist patterning and wet-etch oxide. The features were etched using DRIE. The detection channel was 0.5 um deep; the remaining channels were 4 um deep. A standard coverslip was used as the fourth wall (or "ceiling") of the flowcell. The flowcell was assembled by preparing the coverslip with a water rinse and oxygen plasma treatment in a plasma oven (PLASMA-PREEN, model H937, Plasmatic Systems, Inc., North Brunswick, NJ).

*2.3 Pressure/voltage controller*

A custom pressure and voltage controller (Fig. 5) was designed to interface with the microfluidics flowcell. The controller consists of six channels of polyethylene tubing (as an air guide) through which 30 gauge platinum wire electrodes run (for voltage control). All channels are capable of bipolar voltage output up to +/- 2000V at 50 µA. The front of the controller includes digital displays to indicate the voltage across (resolution of +/- 1V) and current through (resolution less than 10 nA) each electrode.

All six channels are capable of independent pressure control from a gas source. The channels have the ability to regulate pressure into a closed head space from near zero gauge to a full scale value of 10 kPa, gauge pressure or relative to atmosphere. The resolution on each channel is 10 Pa.

Fig. 5. Custom voltage/pressure controller. Left, front panel showing six channels. Right, PDMS-molded channel terminus showing platinum electrode.

For automated bead trapping work, a wheel flowcell was viewed with an optical microscope (Zeiss Axiovert S100TV, Carl Zeiss Inc., Jena, Germany). All ports of the flowcell were loaded with a buffer solution. The buffer solution was 0.1% TWEEN, 10 mM Tris (pH 7 – 7.8) 1 X BSA, 0.1 mM EDTA, filtered slowly through a 0.02µ syringe filter (so as not to create air bubbles). Into one port were introduced polystyrene beads. Beads were tested in concentrations from 100 to 100,000 / mL. The video image was monitored by an image capture program in LabView (IMAQ, National Instruments, Austin, TX). In-house custom software was written to automatically find, track, and position the beads into individual traps. All computations were performed on a PC (1.8 GHz main processor, 1 Gb RAM, ATI Radeon AGP graphics card).

Theoretical pressures and electric fields present in the flowcell were modeled with computational fluid dynamics software (CoventorWare; Coventor, Inc., Cary, NC).

*2.4 Bead Tracking Algorithms*

The automated procedure breaks down into three parts: 1) Find the locations of the bead traps in terms of (x,y) image coordinates; 2) Find the current position of the bead; and 3) Move the bead to the specified bead trap position.

#90526 - $15.00 USD Received 6 Dec 2007; revised 23 Jan 2008; accepted 25 Jan 2008; published 29 Feb 2008

Initial finding of wheel position: No special assumption was made regarding the position and orientation of the flowcell in the microscope image, except that it match a known template, which is consistent with the final design. The (x,y) position and angular orientation are separate problems. We took advantage of the prominence of the circular wheel feature. This allowed us to first find the (x,y) location of the central wheel structure, and then its angular orientation [Eq. (1)]. We experimented with a "brute force" 2D cross-correlation with a "gold standard" image, but this was found to take too much processing time. Using the Fourier relationship [14],

$$f(x,y) \otimes g(x,y) \leftrightarrow F(u,v)\Im\{g(-x,-y)\}, \quad (1)$$

transforms of the standard and experimental images were used to more efficiently compute the cross-correlation.

Initially it was seen that static blemishes in the optical path overwhelmed the true result due to large contrast differences. Since the features are inherently low-contrast, we performed an edge-detection algorithm [15] on the sample image [Fig. 6(a)], which improved contrast while reducing image information. We decided to work with a designed template consisting of only the center wheel feature, which further reduced complexity. Finally, working in the Fourier domain to perform correlation reduced the required time significantly. The resulting cross-correlation result [Fig. 6(b)] is robust.

*2.4.1 Wheel angle*

Cross-correlation will find the Cartesian position of the wheel, but the angle of the image needs to be determined for proper tracking. A Radon transform [16] was used to determine the angle of the straight lines in the binary-thresholded image. Since the main flush channel is so prominent, the Radon transform can robustly find it in a sub-image containing only the center of the flowcell [Fig. 6(c)]. The flowcells are made from the same silicon master; therefore, the channel and bead trap locations are the same from flowcell to flowcell. Thus, the wheel position and angle is sufficient to locate the other channels and bead traps.

*2.4.2 Bead location and tracking*

During trap experiments, once a bead came into the field of view, a cross-correlation technique similar to wheel finding was used to locate the bead. The bead was found in a similar manner to the wheel structure. A circular binary template was created from the known bead size (3 μm). The bead is the only structure in the image with this shape, so another Fourier correlation operation quickly finds the bead. The correlation "knows" where to start looking since it has stored the location of the inlet channel. After initial bead location, the bead position was continuously monitored by determining the intensity centroid in a kernel twice the bead size, centered at its last known position. This operation is faster than full 2D cross-correlation because it assumes the bead has not moved very far from the last frame, so a smaller kernel may be used.

*2.4.3 Bead position control*

A velocity controller with feedback [17] implemented in LabView (National Instruments, Austin, TX) was used to position the bead. For purposes of one-bead docking, one pressure channel (controlling the fluid motion around the wheel) was sufficient to change the bead position. The bead is assumed to be located within the main wheel structure, such that its position can be characterized by its angular distance from the most-distal bead trap about the center of the wheel. The pressure differential in the bead loading channel was also monitored and controlled. As the bead approached the wheel rim, another LabView routine continuously calculated the angular location of the bead relative to the drain channel. Frame-to-frame differences provided the angular velocity of the bead. The locations of the ten bead traps are

#90526 - $15.00 USD Received 6 Dec 2007; revised 23 Jan 2008; accepted 25 Jan 2008; published 29 Feb 2008

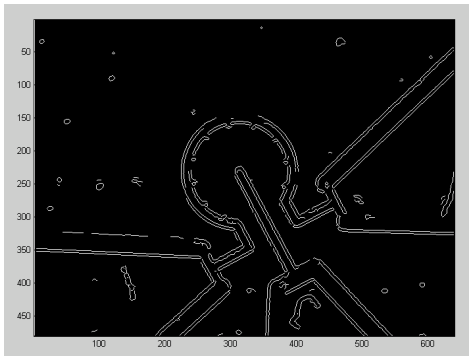

(Fig. 6a)

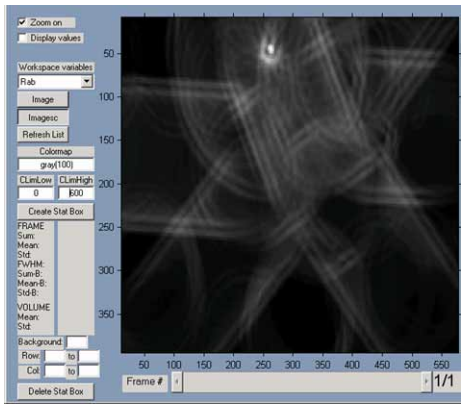


(Fig. 6b)

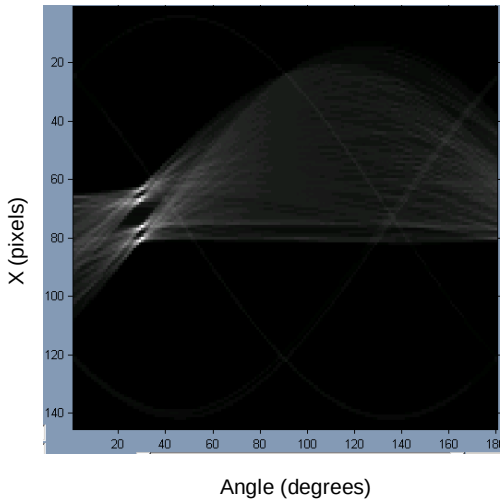


(Fig. 6c)

Fig. 6. Image processing. Flowcell image after edge detection (a), Cross-correlation result of binary-thresholded images (b), Result of Radon transform on binary-thresholded flowcell image (c).

#90526 - $15.00 USD Received 6 Dec 2007; revised 23 Jan 2008; accepted 25 Jan 2008; published 29 Feb 2008

known once the wheel has been located, such that a user may enter a desired bead trap by number from a drop-down list.

Upon selection of a bead trap, the program utilizes a velocity-feedback loop to control the angular position of the bead [Eq. (2)]. The change in pressure was controlled by the error between target and actual velocity,

$$\frac{d}{dt}p(t) = K\left(v_a(t) - v_t(t)\right) \tag{2}$$

where $p$ is the pressure difference between source and drain channels, $v_a$ is actual velocity, $v_t$ is target velocity, and $K$ is a user-adjustable gain. The target velocity was determined by a sigmoidal relationship [Eq. (3)]:

$$v(t) \propto \frac{1-e^{-\alpha\theta}}{1+e^{-\alpha\theta}} \tag{3}$$

where $\theta$ is the difference between the actual angle and the target angle, and $\alpha$ is a user-adjustable slope parameter. The sigmoid relationship permits a high initial velocity with steadily decreasing velocity as the bead approaches the target position, from either side. Collectively, the algorithms essentially comprise a proportional-integral (PI) controller.

## 3. Results and discussion

### *3.1 Flowcell handling*

During the course of multiple experiments with loading and manipulating beads, several flowcell handling procedures were developed. These comprise the "art" of the experiments and may be useful to others. Thus, we report on them briefly here. First, a deionized water rinse and plasma treatment is often sufficient for preparing the coverslip side of a PDMS flowcell. In our treatment, washing was done near a laminar flow hood and dried with compressed nitrogen gas under the hood. The plasma treatment both cleans and oxygenates the coverslip surface, facilitating covalent bonding between oxygen and silicon atoms.

Second, with multiple beads intended to be docked simultaneously, the order of bead loading becomes important. The channel size differential at the bead trap location creates a bulk fluid flow velocity differential across the trap. The resulting three-dimensional pressure differential decreases by the inverse square of distance from the trap. Therefore, bringing the bead in close proximity to the trap helps "draw" it into the trap. Once the bead is set in the trap, it will not easily dislodge (typically, at least a threefold increase in main channel pressure was required for inadvertent dislodging). Moreover, with the bead set in place, the trap is closed and the pressure differential disappears, permitting subsequent beads to flow past the trap without being directed towards it. In the final loading scheme for a particular application, it may thus be easiest to bring in the first bead to the nearest port then load back to the furthest port. However, with careful pressure control, we were able to load beads in any order.

Third, evaporation at the loading well will obviously greatly disrupt pressure flow control. It is therefore important to not allow buffer to evaporate from the flowcell with beads loaded. This can easily be accomplished by periodically replenishing the buffer solution. An ultrasonic bath can assist in dislodging beads stuck in channels or bead traps.

### *3.2 Manual bead docking*

Manual bead docking was routinely achieved with pressures under 3000 Pa for loading, 1000 Pa for retention, and 10000 Pa for flushing, all of which were within the specifications of the controller. Typical channel pressures in the flowcell are shown in Fig. 7, with modeled flow

#90526 - $15.00 USD Received 6 Dec 2007; revised 23 Jan 2008; accepted 25 Jan 2008; published 29 Feb 2008

rates overlaid on the channels. An experienced operator can load 10 beads in under 10 minutes. Figure 8 shows an example of ten docked beads in a silicon-Pyrex flowcell.

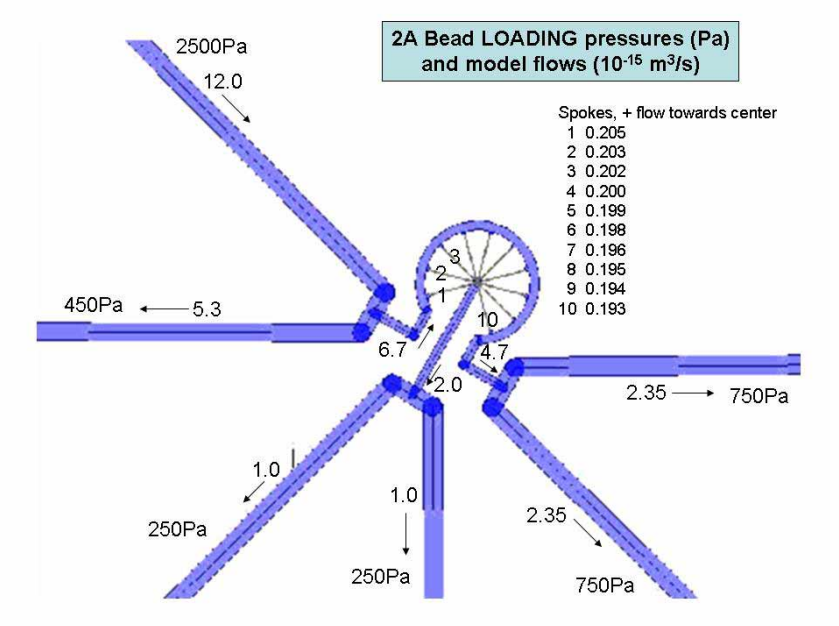


Fig. 7. Typical bead loading pressure settings. Numbers marked in Pa are pressures, and unlabeled numbers with accompanying arrows are volume flow rates in $10^{-15}$ $m^3/s$. Unlabeled numbers over wheel spokes show spoke numberings. See Materials and Methods for description of flowcell design.

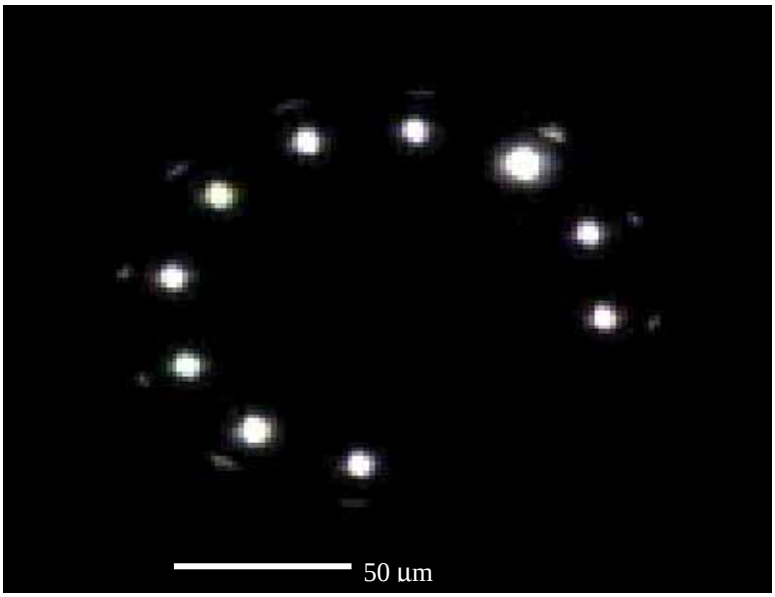


Fig. 8. Bead docking. CCD fluorescence image of 10 beads docked within a wheel flowcell.

#90526 - $15.00 USD Received 6 Dec 2007; revised 23 Jan 2008; accepted 25 Jan 2008; published 29 Feb 2008

Electrophoretic extension of DNA was achieved with electric fields below 50 V/cm. Examples of both functions are shown in Fig. 9. The electric field is applied down the narrow (vertical) channel (which the bead cannot enter due to size), pulling the DNA into the channel and extending it down the channel, creating a "ponytail" that can be seen in the image.

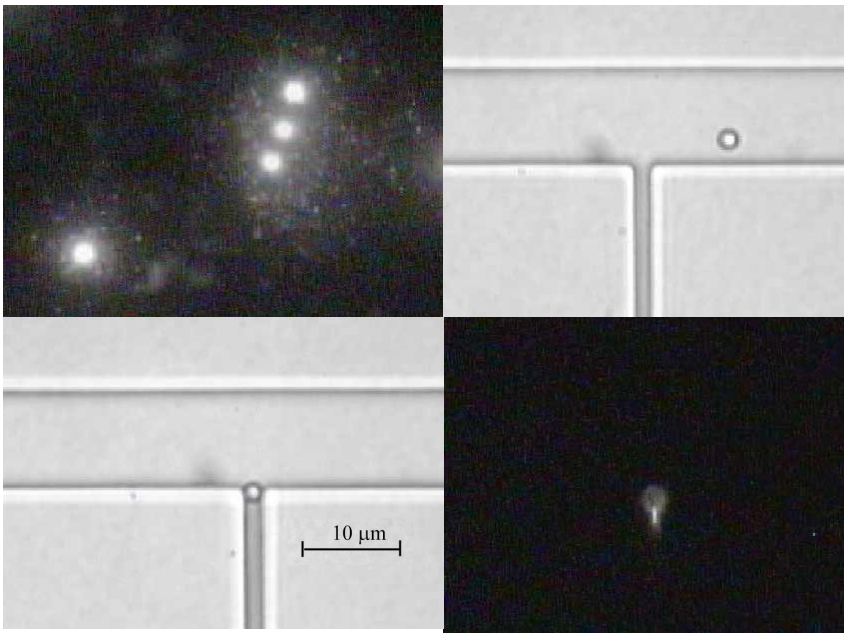


Fig. 9. Images from bead-trapping experiment. Top left, fluorescence imaging of several beads, each with many DNA strands attached. Top right, brightfield image of bead approaching bead trap. Bottom left, brightfield image of bead trapped at intersection. Bottom right, fluorescence image of bead trapped at intersection with electric field extending DNA into the channel.

### *3.3 Automated bead docking*

Experimentation showed that the automated algorithm was able to control bead velocity with angular speeds up to 40 degrees/second. This velocity corresponds to about a 400 Pa difference of the bias pressure in either direction. The final time to find the (x,y) location of the flowcell was about 3 seconds, which is reasonable in a real-time system since it only needs to be done once. The time for initial location of the bead once it has entered the microscope field of view was under 1 second. Finally, once the bead is introduced to the wheel rim channel, it can be positioned to a desired bead trap in a few seconds.

## 4. Conclusions

We have demonstrated a microfluidics platform capable of bead handling, position control, and DNA extension using pressures and electric fields easily generated in the laboratory. An automated software algorithm was presented that is able to reversibly dock and undock a bead in a microchannel. The platform is suitable for experiments with quickly-produced prototypes (PDMS), or with a more permanent flowcell material (silicon/Pyrex).

#90526 - $15.00 USD Received 6 Dec 2007; revised 23 Jan 2008; accepted 25 Jan 2008; published 29 Feb 2008